CHAPTER 13

TERNARY THREE-PHASE EQUILIBRIUM

Three-phase equilibrium in ternary systems occurs over a *temperature range* and not, as in binary systems, at a single temperature. It is bivariant:

$$P + F = C + 2$$
$$3 + 2 = 3 + 2$$

After the pressure has been established, only the temperature, or one concentration parameter, may be selected in order to fix the conditions of equilibrium. The representation of three-phase equilibrium on a phase diagram requires the use of a structural unit which will designate, at any given temperature, the fixed compositions of three conjugate phases. Such a structural unit is found in the tie-triangle.

Tie-triangles

If any three alloys of a ternary system are mixed, the composition of the mixture will lie within the triangle produced by connecting the three original composition points with straight lines (Fig. 13-1). For example, take three compositions R, S, and L as follows:

$$R = 20\%\ A + 70\%\ B + 10\%\ C$$
$$S = 40\%\ A + 40\%\ B + 20\%\ C$$
$$L = 10\%\ A + 30\%\ B + 60\%\ C$$

and mix two parts of R with three parts of S and five parts of L:

$$0.2 \times 20 + 0.3 \times 40 + 0.5 \times 10 = 21\%\ A$$
$$0.2 \times 70 + 0.3 \times 40 + 0.5 \times 30 = 41\%\ B$$
$$0.2 \times 10 + 0.3 \times 20 + 0.5 \times 60 = 38\%\ C$$

The total composition ($21\%\ A + 41\%\ B + 38\%\ C$) is seen to lie *within* the triangle RSL at point P, Fig. 13-1. No matter what proportions of the three alloys had been taken, the same would have been true.

Once more the lever principle can be applied. This time the lever is the weightless plane triangle RSL supported on a point fulcrum at P. If 20%

of the alloy R is placed upon point R, 30% of alloy S upon point S, and 50% of alloy L upon point L, then the lever plane will balance exactly. For purposes of calculation it is convenient to resolve the planar lever into two linear levers such as SPO and ROL, Fig. 13-1, by drawing a straight line from any corner of the triangle through point P to its intersection with the opposite side. The quantity of the S alloy in the mixture P is then

$$\%S = \frac{PO}{SO} \times 100 \qquad \text{and} \qquad \%O = \frac{SP}{SO} \times 100$$

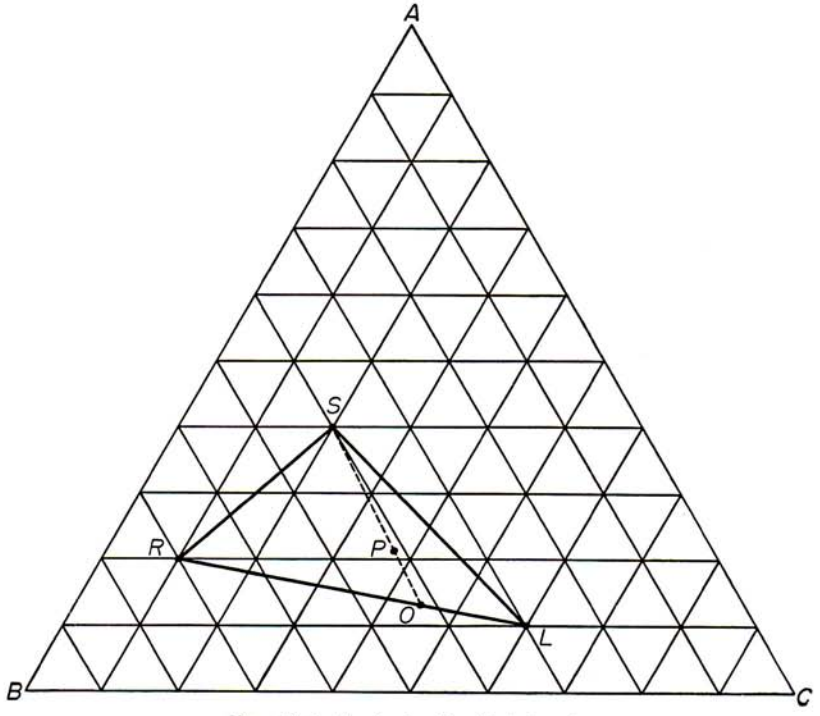

FIG. 13-1. Analysis of a tie-triangle.

Composition O represents the mixture of alloys R and L, so that

$$\%R = \frac{OL}{RL}\frac{SP}{SO} \times 100 \qquad \text{and} \qquad \%L = \frac{RO}{RL}\frac{SP}{SO} \times 100$$

By measuring the line SPO, it is found that the segment SP is 18.2 mm long and the segment PO is 7.8 mm long. Thus, the mixture P contains

$$\%S = \frac{7.8}{26} \times 100 = 30\%$$

On the line *ROL*, segment *RO* is 32.85 mm long and segment *OL* is 13.15 mm long, whence

$$\%R = \frac{13.15}{46} \times \frac{18.2}{26} \times 100 = 20\%$$

$$\%L = \frac{32.85}{46} \times \frac{18.2}{26} \times 100 = 50\%$$

The triangle *RSL* may be employed as a tie-triangle connecting three phases which associate to form an intermediate gross composition or phase or, conversely, three phases into which *P* decomposes. There are then two kinds of "tie-elements" that appear in ternary diagrams, namely, the *tie-line* and the *tie-triangle.*

Three-phase Equilibrium in the Space Model

A simple example of three-phase equilibrium in a ternary system is shown in Fig. 13-2. One of the binary systems involved in this ternary system is isomorphous; the other two are of the eutectic type. There are three one-phase regions: L, α, and β; three two-phase regions: $L + \alpha$, $L + \beta$, and $\alpha + \beta$; and one three-phase region: $L + \alpha + \beta$. These are shown individually in the "exploded model," Fig. 13-3. Edges of regions that meet to form a common line in the assembled diagram are labeled with identical numbers in the exploded model.

Each of the two-phase regions is like a piece cut out of the $L + \alpha$ region of the isomorphous diagram discussed in the preceding chapter. It has two bounding surfaces which are connected at every point by tie-lines joining the conjugate phases. Thus, the $L + \alpha$ region of Fig. 13-3 exhibits a liquidus surface on top and a solidus surface beneath (dotted outline); its form can be seen in the matching top face of the α region shown just below. Tie-lines join every point on the liquidus with a corresponding point on the solidus. The other exposed surfaces of the $L + \alpha$ region are portions of the confining walls of the space diagram. On its underside the $L + \alpha$ region has a "ruled surface" (dotted outline) formed by the tie-lines (dotted) that join the edge of the liquidus 4 with the edge of the solidus 3. This surface is identical with one of the top surfaces of the $L + \alpha + \beta$ region 1-2-3-4. The $L + \beta$ region is entirely similar and its undersurface is identical with the other top surface of the $L + \alpha + \beta$ region 1-2-4-5. Beneath the three-phase region is the field of $\alpha + \beta$, which is bounded by two solvus surfaces that are connected at all points by tie-lines joining the conjugate α and β phases. The top surface of the $\alpha + \beta$ region is generated by tie-lines connecting the edges 3 and 5. This surface is identical with the bottom surface of the $L + \alpha + \beta$ field, 1-2-3-5, not visible in the drawing (dotted tie-lines).

From this it can be seen that the three-phase region $L + \alpha + \beta$ is enclosed by three surfaces, each composed of tie-lines. At any one temperature, the tie-lines on the three surfaces meet to form a triangle, which is a tie-triangle. Just as each two-phase field is composed of a "bundle of tie-lines," the three-phase field is composed of a "stack of tie-triangles" (see Fig. 13-4). At each end of the field the last triangle is closed to a single line (the binary eutectic line), so that the region has only three surfaces, all of which meet at sharp edges on all sides. Although generated by horizontal straight lines (tie-lines), the three bounding surfaces are not

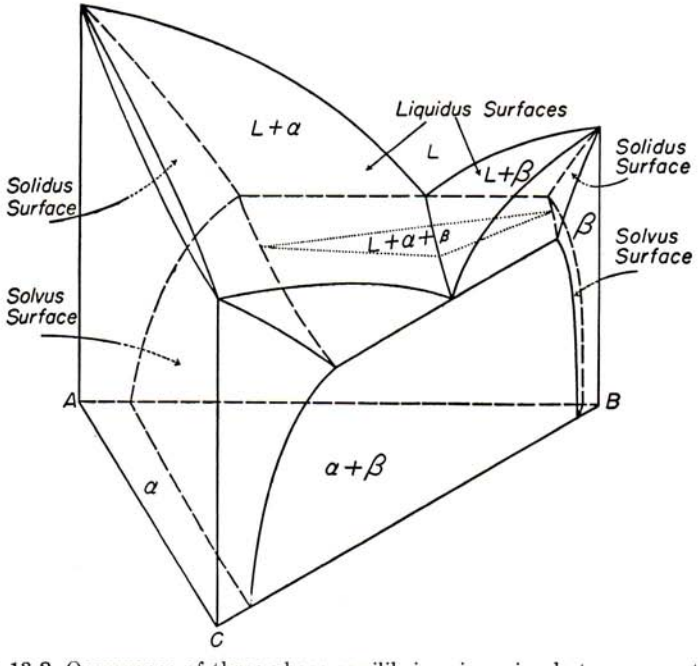

FIG. 13-2. Occurrence of three-phase equilibrium in a simple ternary system.

plane, because the tie-lines turn as they descend in temperature, producing curved ruled surfaces. The vertices of the tie-triangles lie on three conjugate lines labeled α, β, and L in Fig. 13-4. By reference to Figs. 13-2 and 13-3 it can be seen that the respective one-phase fields terminate on these lines. Thus, at each temperature level, three-phase equilibrium is represented by a tie-triangle the corners of which touch the three one-phase regions at composition points that are unique and the sides of which are in contact, respectively, with the three two-phase fields.

These details are perhaps best represented by the use of isothermal sections, Fig. 13-6, where the five isotherms are taken at the temperatures designated T_1 to T_5 in Fig. 13-5. Returning to the requirements of the

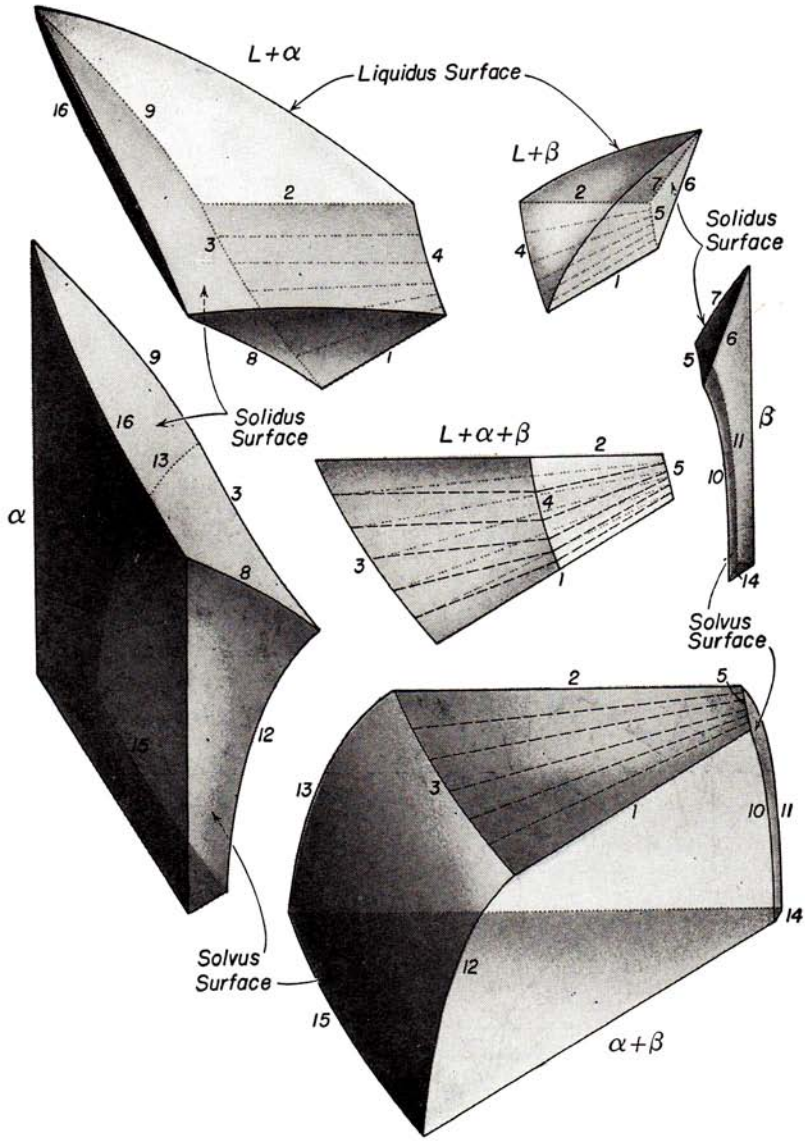

FIG. 13-3. Exploded model of the diagram of Fig. 13-2.

phase rule, with which this chapter was opened, it is now a simple matter to demonstrate that the one degree of freedom remaining after the establishment of a fixed pressure is sufficient to complete the definition of all variables in three-phase equilibrium. If a specific temperature is chosen, say T_2 in Fig. 13-6, then the compositions of all of the three conjugate

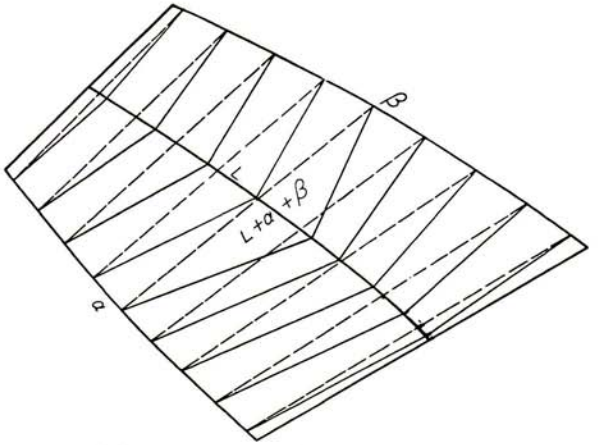

FIG. 13-4. A region of three-phase equilibrium in temperature-composition space.

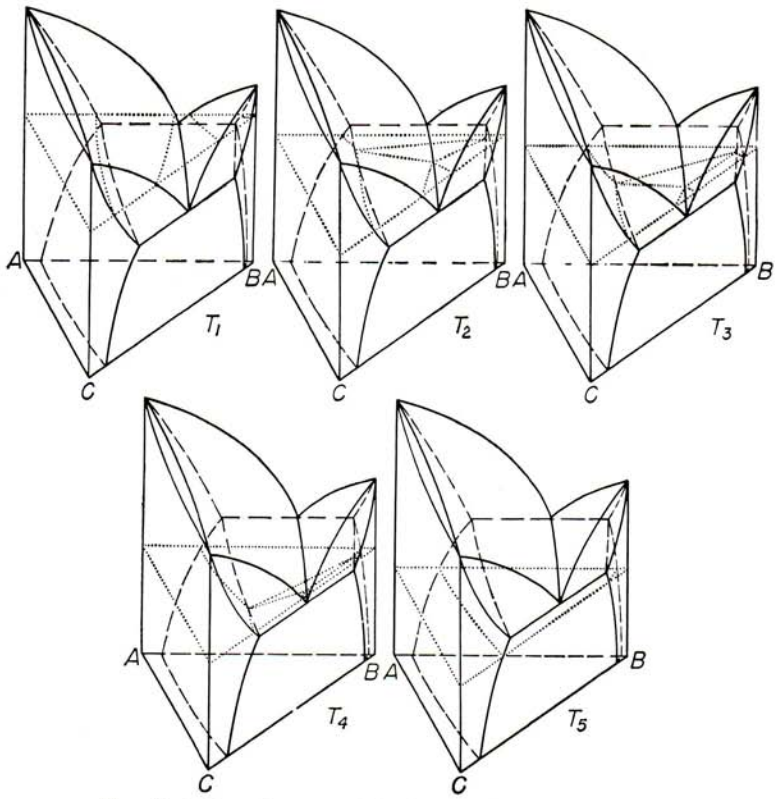

FIG. 13-5. Development of isotherms shown in Fig. 13-6.

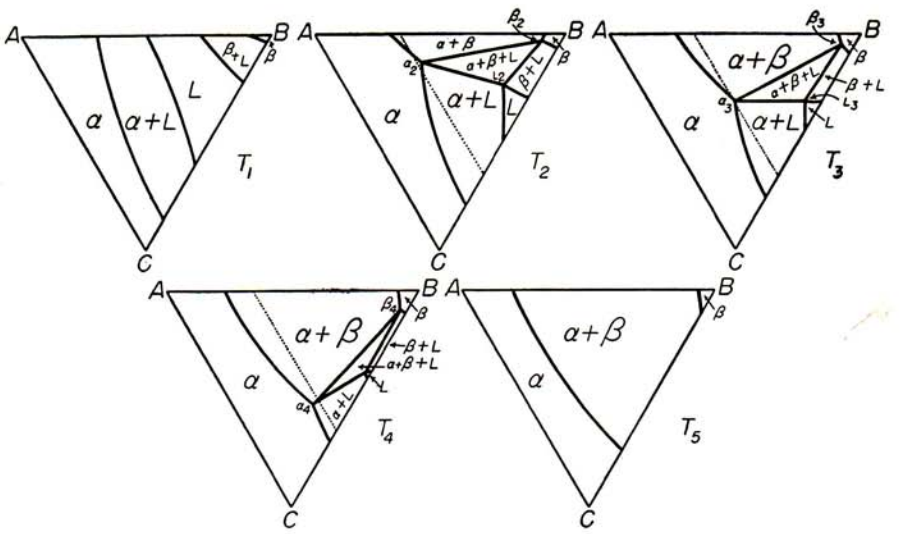

FIG. 13-6. Isotherms through the space diagram of Fig. 13-2.

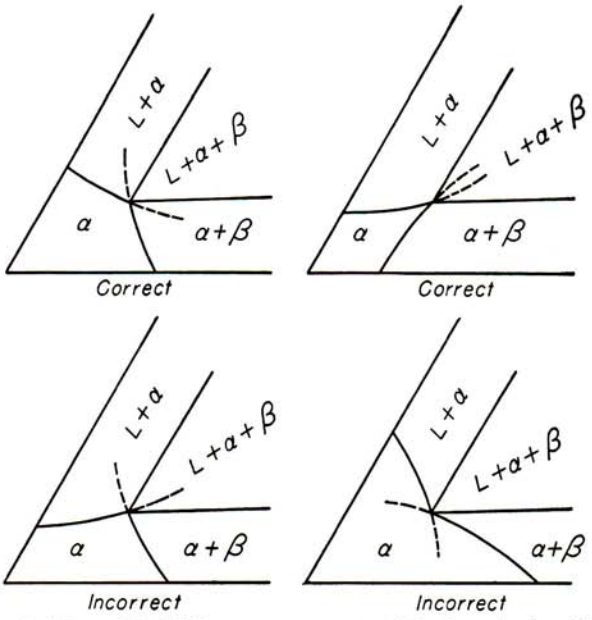

FIG. 13-7. Permissible and forbidden arrangements of the boundaries of the one-phase field.

phases are fixed, respectively, at α_2, β_2, and L_2. Or similarly, if a concentration parameter is defined by requiring that the α phase in equilibrium with β and L shall contain 35% B (indicated by the dotted line in isotherms T_2, T_3, and T_4), there will be only one isotherm (T_3) in which this condition is realized. The temperature and the compositions of the conjugate β_3 and L_3 phases are fixed by establishing one concentration parameter of α.

The principle of the minimum free energy leads to a helpful limitation on the construction of the three-phase region, illustrated in Fig. 13-7. Boundaries between the one- and two-phase fields, where they meet the three-phase field, may either *both* project into different two-phase fields or *both* project into the three-phase field, but it is *not correct* for one of a pair of boundaries to project into a two-phase field and the other into the three-phase field or for either or both to project into the one-phase field.

Freezing of an Alloy

Before considering the course of natural freezing of an alloy involving ternary three-phase equilibrium, it will be instructive to follow the corresponding path of "equilibrium phase change." This can be done most satisfactorily by reference to a series of isotherms (Fig. 13-8). The circled cross designates in each isotherm the gross composition X of the alloy under observation. At temperature T_1 (the first isotherm) the X composition lies in the liquid field and the alloy is fully molten.

At T_2, the next lower temperature represented, freezing is just beginning. Composition X lies upon the liquidus and is joined with the first solid to appear by the tie-line $L_2\alpha_2$.

At T_3 a substantial quantity of α is present:

$$\%\alpha_3 = \frac{XL_3}{\alpha_3 L_3} \times 100 \approx 20\%$$

and

$$\%L_3 = \frac{\alpha_3 X}{\alpha_3 L_3} \times 100 \approx 80\%$$

At T_4, as the gross composition passes into the $L + \alpha + \beta$ field, the first particles of the β phase begin to appear; the α and β now crystallize simultaneously from the liquid.

At T_5 all three phases are present in substantial quantity:

$$\%\alpha_5 = \frac{XS_5}{\alpha_5 S_5} \times 100 \approx 60\%$$

$$\%\beta_5 = \frac{L_5 S_5}{L_5 \beta_5} \frac{\alpha_5 X}{\alpha_5 S_5} \times 100 \approx 20\%$$

and

$$\%L_5 = \frac{S_5 \beta_5}{L_5 \beta_5} \frac{\alpha_5 X}{\alpha_5 S_5} \times 100 \approx 20\%$$

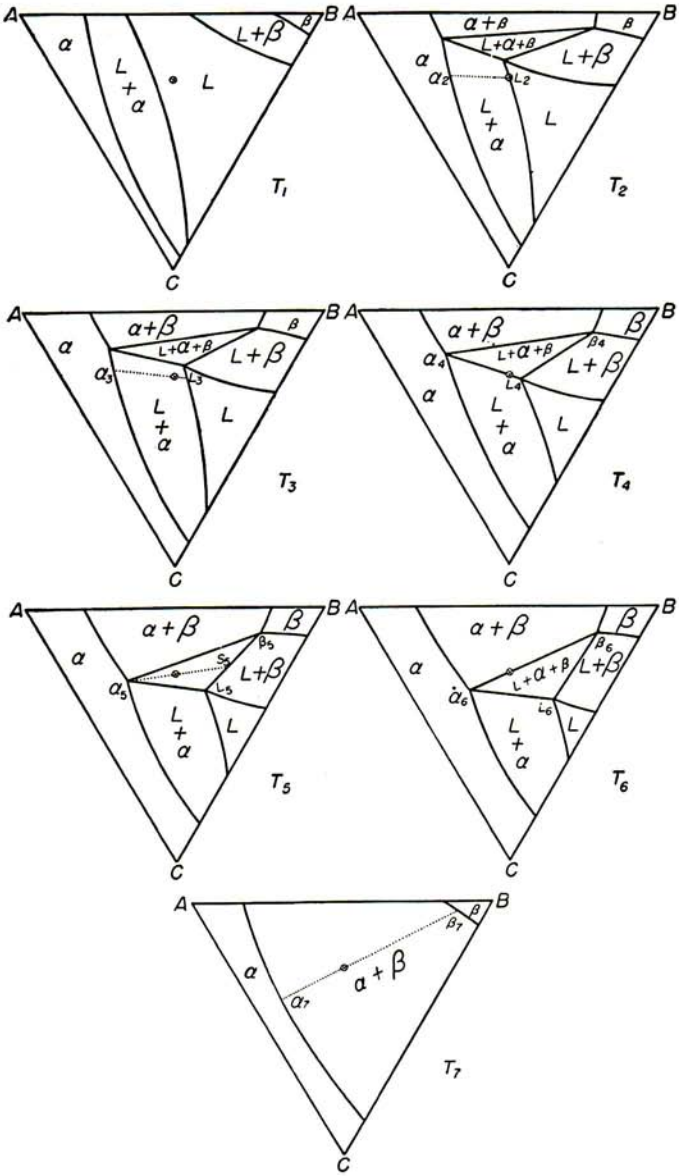

FIG. 13-8. Illustrating the sequence of equilibria involved in the freezing of an alloy whose gross composition is indicated by the circled cross in each isotherm.

At T_6 the last of the liquid disappears and there remains only

$$\%\alpha_6 = \frac{X\beta_6}{\alpha_6\beta_6} \times 100 \approx 75\%$$

and

$$\%\beta_6 = \frac{\alpha_6 X}{\alpha_6\beta_6} \times 100 \approx 25\%$$

At T_7 the compositions of the two solid phases have changed slightly in response to the curvature of the α and β solvus surfaces, and their relative proportions will again be given by the tie-line $\alpha_7\beta_7$.

Freezing has proceeded in two steps, neither of which is isothermal; primary freezing of the α phase has been followed by a secondary separation of $\alpha + \beta$ over the temperature range T_4 to T_6. This process is illustrated schematically in Fig. 13-9, which represents the freezing of a lead-antimony-bismuth alloy (90% lead + 5% antimony + 5% bismuth), the constitution of which is given by the space diagram in Fig. 13-10 and the isotherms in Fig. 13-11. The first five pictures of Fig. 13-9 are sketches showing the presumed progress of freezing at the temperatures indicated and corresponding to the requirements of the isotherms at the same temperatures, Fig. 13-11, where the gross composition of the alloy is indicated by the point X in each section. The sixth picture ("20°C") is an actual photomicrograph of this alloy. Large white areas represent the liquid phase, unbroken black areas the primary α, and black mixed with white designates the α (black) and β (white) of the secondary constituent. At 300°C the primary crystallization of α (black specks) has just begun, and at 235°C these particles have achieved their maximum growth. Thereafter α and β crystallize together, so that at 230°C more than half of the remaining liquid has been converted to the secondary two-phased solid constituent. Freezing is complete at 225°C, the only subsequent change being a slight increase in the volume of the β, at the expense of α, as the compositions of the solid phases change along the solvus. The final microstructure, at 20°C, is not visibly different from that of a binary hypoeutectic alloy, but the manner of its formation differs in that the secondary constituent (the "eutectic constituent") has grown over a range of temperature instead of isothermally.

Wherever transformation occurs over a temperature range at a finite rate (i.e., natural freezing), it is anticipated that the products of that transformation will exhibit the *coring effect*. Thus, both the primary and secondary constituents, in the above example, should be cored. Coring of the primary constituent has been described in the preceding chapter; the primary α phase of the present example will freeze in the same manner as the α phase of an isomorphous system. When α and β are crystallizing together, both phases should be cored (see Fig. 13-12). On this diagram, "equilibrium" freezing would begin at T_1, where x_1 falls on the line

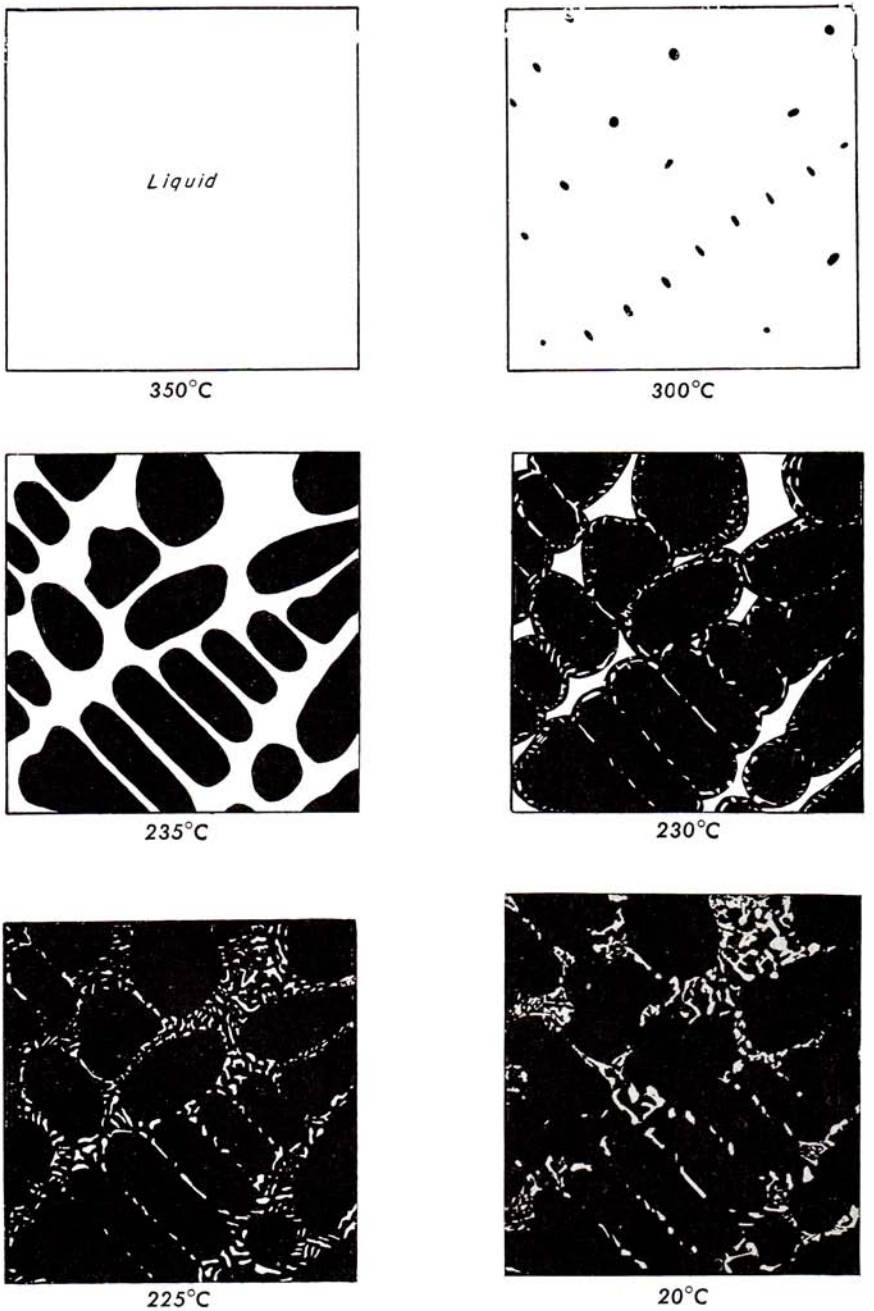

FIG. 13-9. Schematic representation of the progress of freezing of an alloy composed of 90% Pb + 5% Bi + 5% Sb, indicated by point x in Fig. 13-11. The first five pictures of the series are idealized sketches; the sixth picture is an actual photomicrograph of the alloy at room temperature. Magnification 100.

$L_1\alpha_1$, and would end at T_3, where x_3 falls on the line $\alpha_3\beta_3$. The α and β phases fail to maintain equilibrium composition in natural freezing,[1] however, and their average compositions follow the lines: $\alpha_1\alpha_2'\alpha_3'\alpha_4'$ and $\beta_1\beta_2'\beta_3'\beta_4'$, respectively. Therefore, at T_3 some liquid remains, because x_3 lies within the triangle $L_3\alpha_3'\beta_3'$. At T_4 the gross composition point x_4 finally lies upon the line $\alpha_4'\beta_4'$, and crystallization is completed. This temperature is well below the final temperature of equilibrium freezing, and the composition of the last layer of each solid phase (α_4 and β_4) lies far to the right of the gross composition point. Coring of the secondary $\alpha + \beta$

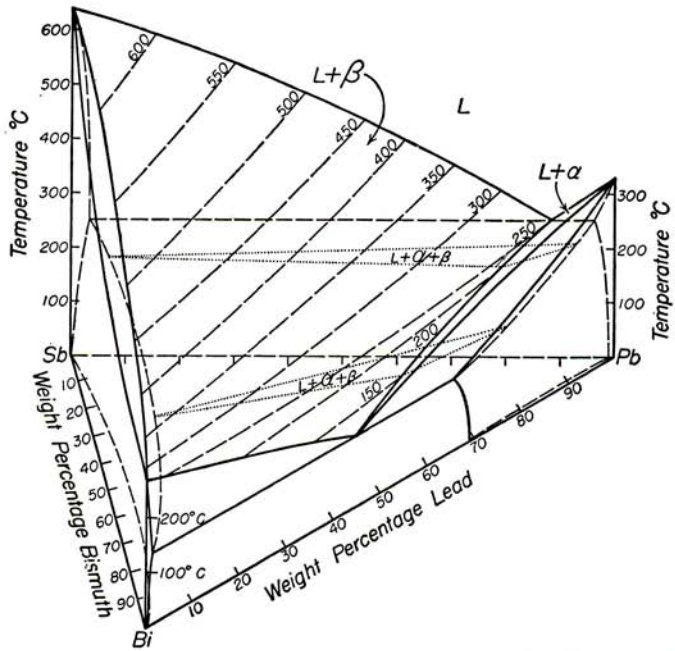

FIG. 13-10. Temperature-composition diagram of the system lead-bismuth-antimony.

constituent, although necessarily present, is rarely observed in the microstructure, partly because of the fineness of the particles into which the two phases are divided. When coring of the primary constituent precedes coring of the secondary constituent, the average composition of the solid phase concerned, in both the primary and secondary constituents, will tend toward the initial primary composition. For example, in Fig. 13-12, if the primary constituent is α, the average composition path of the α phase would lie still farther to the left, elongating the $\alpha'\beta'$ side of the tie-triangle. Alloys of gross composition wholly outside the range of the

[1] For simplicity it is assumed again that the equilibrium composition of the liquid phase is maintained.

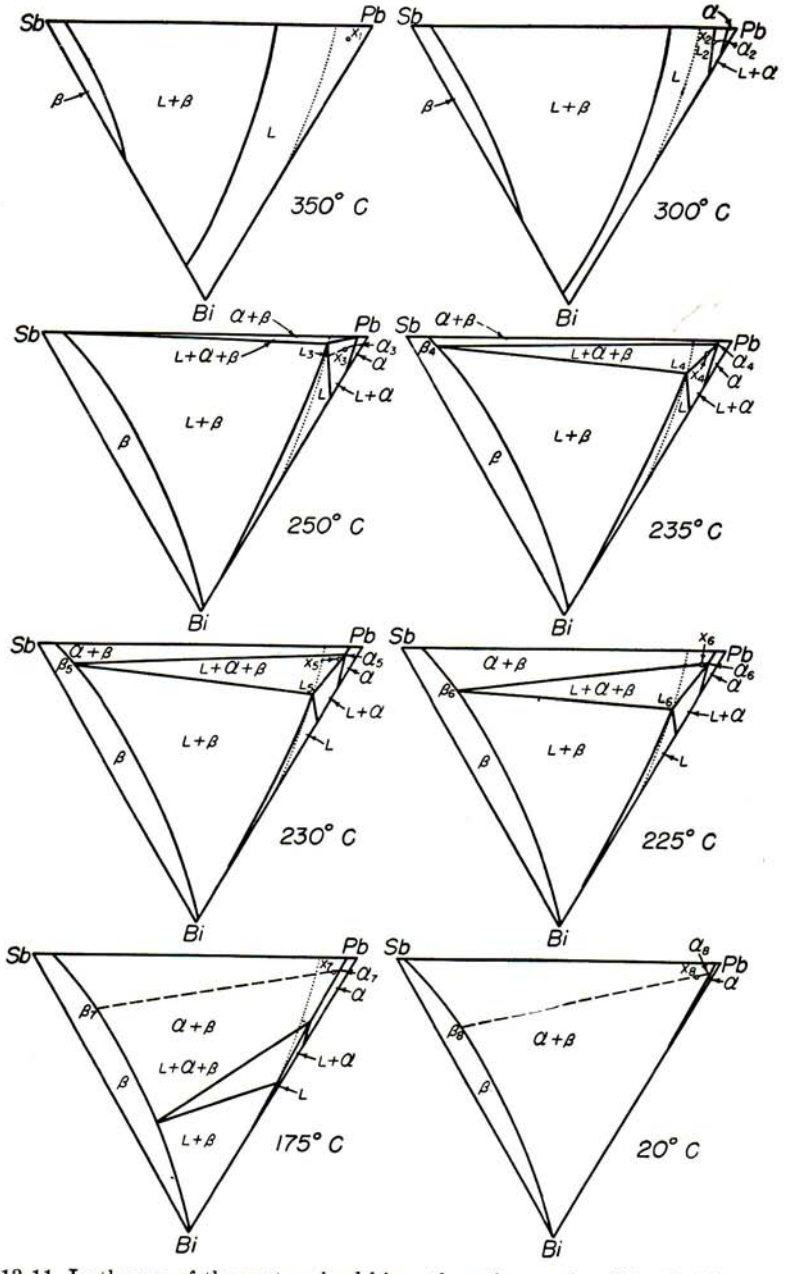

FIG. 13-11. Isotherms of the system lead-bismuth-antimony (see Fig. 13-10).

three-phase field can, therefore, undergo three-phase reaction, just as binary hypoeutectic alloys outside the eutectic range can undergo eutectic reaction.

Heat Treatment

Structural changes accompanying heat treatment may likewise be followed by reference to the isothermal sections. Consider, for example, an alloy which at an elevated temperature, say T_4 in Fig. 13-6, should lie in

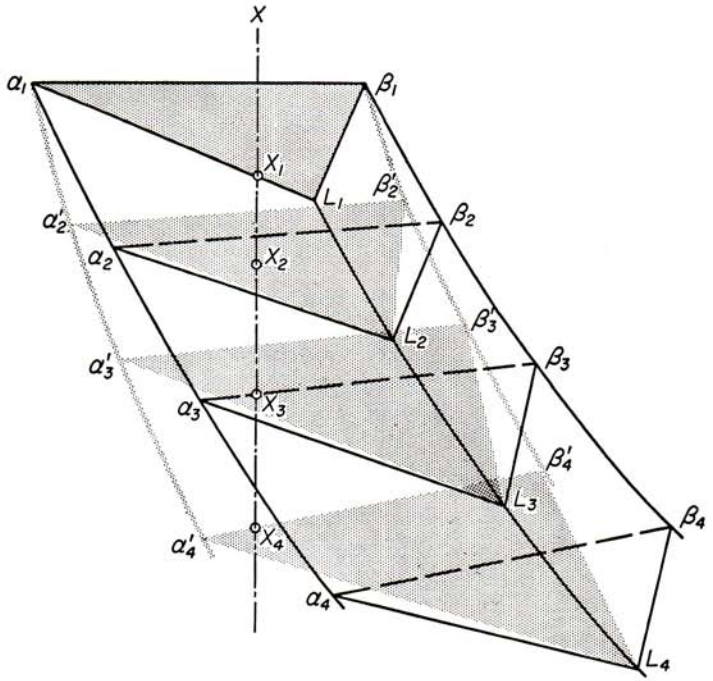

FIG. 13-12. Illustrating the origin of coring in two solid phases (α and β) that freeze simultaneously.

the α field but which, owing to nonequilibrium freezing, contains some of the $\alpha + \beta$ constituent in its structure. This alloy can be converted wholly to α by a homogenizing heat treatment, such as was described in Chap. 4. If at lower temperature this alloy passes into the $\alpha + \beta$ field, then a Widmanstätten precipitate of the β phase will appear during slow cooling to room temperature or upon reheating to an intermediate temperature subsequent to quenching from the homogenizing heat-treating temperature. In almost all respects the process is analogous to that described for the binary case, differing only in that the compositions of the phases con-

cerned lie within the ternary space diagram and must be analyzed by the use of tie-lines which appear in a sequence of isothermal sections.

Another System Involving Three-phase Equilibrium

If two binary peritectic systems are substituted for the two binary eutectic systems of the foregoing example, the resulting ternary space model will appear as in Fig. 13-13. An exploded model of this case is shown in Fig. 13-14. This diagram has the same number of fields as was found in the previous example, and they are similarly designated. The most evident difference is to be found in the $L + \alpha + \beta$ field, which has been inverted to produce peritectic reaction; the trace of the α compositions on this field, line 2 in Fig. 13-14, is on the underside of the three-phase region and, therefore, is dotted in the sketch.

As in the previous example, the one-phase regions touch the three-phase region only along edges, the liquid field along edge 1, the β field along edge 3, and the α field along edge 2. Two-phase regions terminate upon the three surfaces of the three-phase space. The bottom face of the $L + \beta$ region rests upon the top face 1-3-4-5 of the $L + \alpha + \beta$ field. This field is otherwise bounded by liquidus and solidus surfaces and by the confining walls of the diagram. An upper face of the $L + \alpha$ region 1-2-4-5 coincides with one of the two lower surfaces of the $L + \alpha + \beta$ region, and this field is likewise further bounded by the liquidus, solidus, and walls of the diagram. The third surface of the three-phase region rests upon the top face of the $\alpha + \beta$ region 2-3-4-5, which field is otherwise bounded by two solvus surfaces and the walls of the diagram.

These relationships are clearly evident in the isotherms of Fig. 13-15, which should be compared with those of the previous example, Fig. 13-6; it will be seen that the tie-triangles are reversed. The course of freezing may again be followed by the use of the isothermal sections. That peritectic reaction results from the reversal of the tie-triangles can be seen by analyzing the process in detail. Consider first an alloy of composition X shown on tie-triangles at three temperatures in Fig. 13-16. At T_2 the primary separation of β crystals is complete and the precipitation of α is about to begin. The quantity of primary β is

$$\%\beta_2 \text{ (primary)} = \frac{L_2X}{L_2\beta_2} \times 100 \approx 30\%$$

When the temperature falls to T_3, the quantity of β is reduced to

$$\%\beta_3 \text{ (total)} = \frac{mX}{m\beta_3} \times 100 \approx 20\%$$

and this change is accompanied by a corresponding decrease in the quan-

tity of liquid:

$$\%L_2 = \frac{X\beta_2}{L_2\beta_2} \times 100 \approx 70\%$$

$$\%L_3 = \frac{m\alpha_3}{L_3\alpha_3} \frac{X\beta_3}{m\beta_3} \times 100 \approx 60\%$$

and an increase in the amount of the α phase:

$$\%\alpha_2 = 0$$

$$\%\alpha_3 = \frac{mL_3}{\alpha_3 L_3} \frac{X\beta_3}{m\beta_3} \times 100 \approx 20\%$$

Just as in binary peritectic reaction, the primary constituent is consumed by reaction with the liquid to form the secondary constituent. At T_4 the β phase has been consumed altogether and only liquid and α remain.

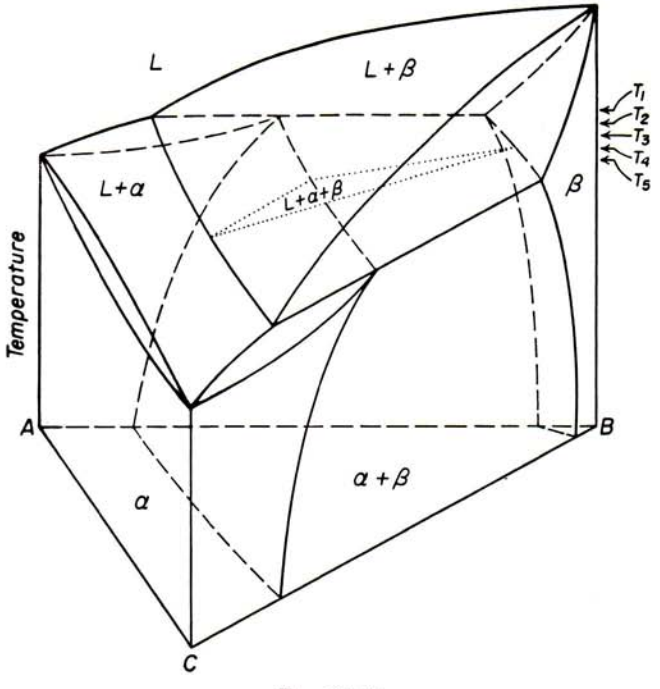

FIG. 13-13

Had the alloy been of composition Y, Fig. 13-16, the same course of events would have been observed, except that all the liquid would have been consumed in forming α, leaving a residue of unreacted β. In natural freezing these processes are retarded by failure to maintain equilibrium. All constituents are cored, envelopment occurs, and the relative quantities of the crystalline phases deviate from the "ideal," just as in binary

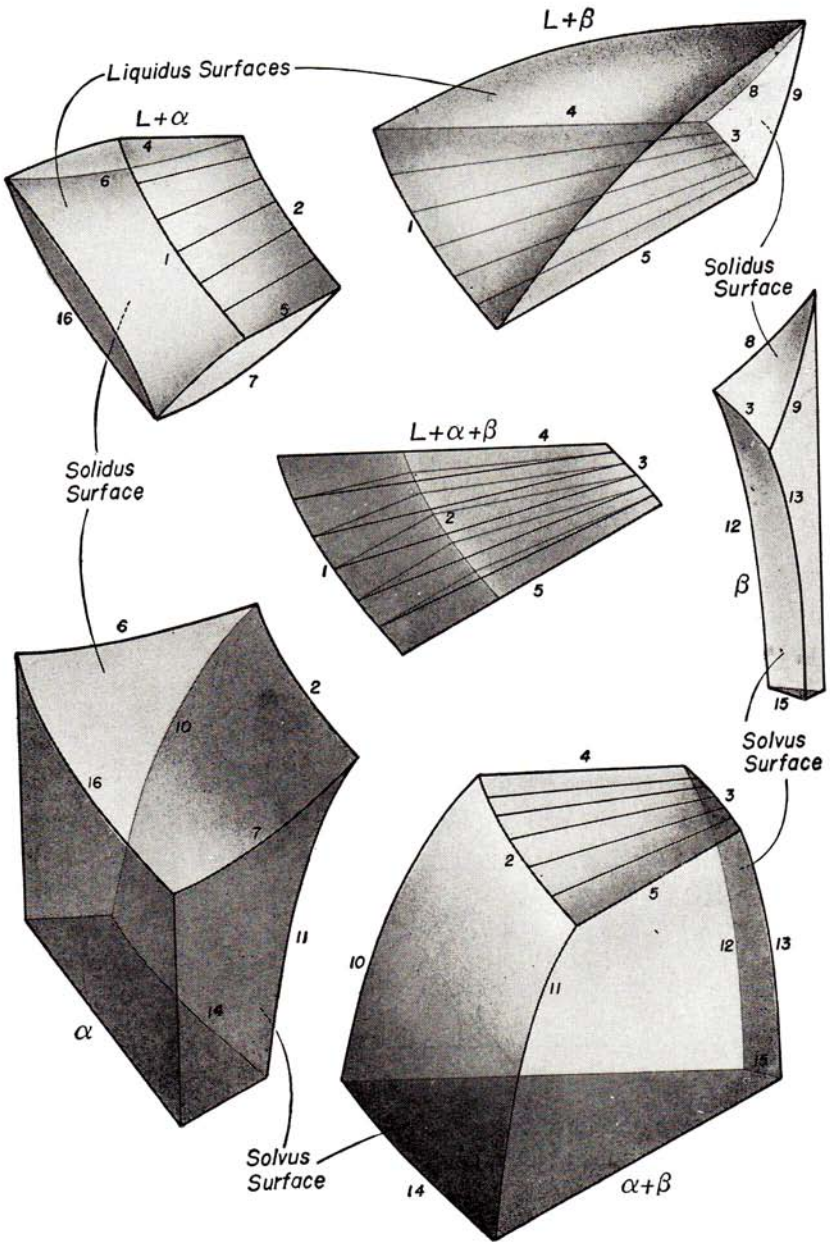

FIG. 13-14. Exploded model of the diagram of Fig. 13-13.

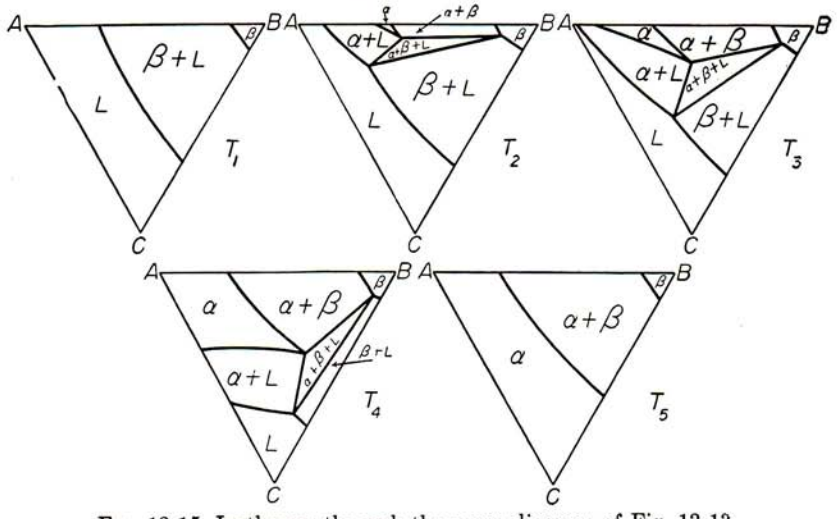

FIG. 13-15. Isotherms through the space diagram of Fig. 13-13.

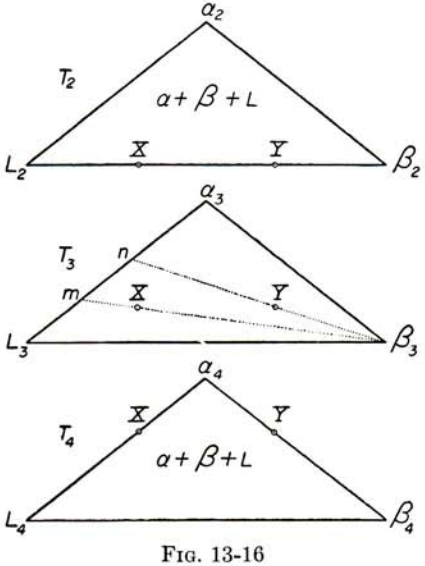

FIG. 13-16

peritectic alloys. The microstructures of cast ternary alloys of this kind are, in fact, indistinguishable from their binary counterparts, the binary peritectic alloys.

Other Kinds of Three-phase Equilibrium

The forms that have been discussed above apply to all cases of three-phase equilibrium. Ternary three-phase eutectoid reaction is represented

by the same construction as is eutectic reaction, simply substituting a solid phase for the liquid. Correspondingly, the monotectic reaction resembles the eutectic case, while the peritectoid and syntectic reactions resemble the peritectic case. *Every isothermal three-phase reaction occurring in any of the binary systems is associated with a corresponding nonisothermal three-phase reaction, described by tie-triangles, in the ternary diagram.*

With any of the above reactions the temperature of ternary three-phase equilibrium may either rise or fall as the gross alloy composition recedes

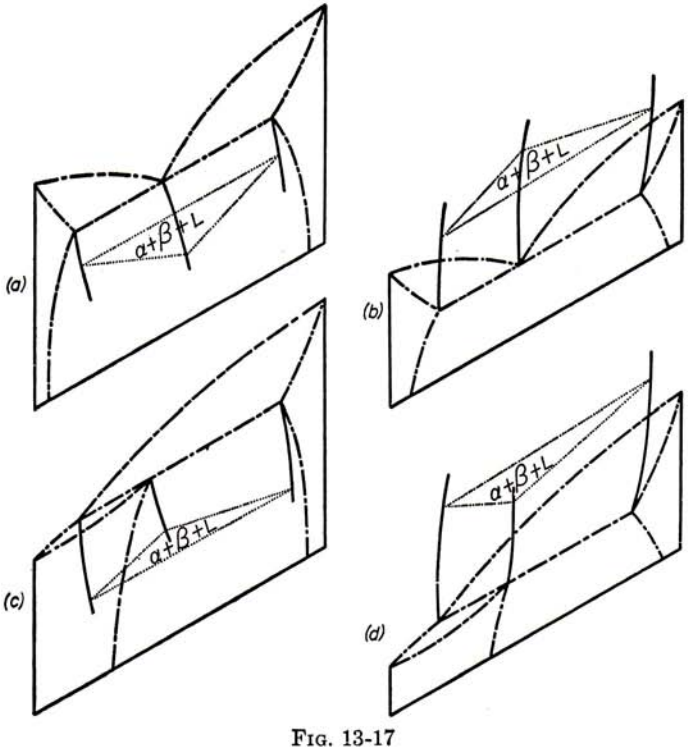

FIG. 13-17

from the binary face of the diagram (Fig. 13-17). If the tie-triangle is considered as an arrow pointing in the direction of the junction of its shorter sides, it may be said that the tie-triangle in eutectic-type reaction points away from the binary face of the ternary diagram if three-phase reaction proceeds to lower temperature, Fig. 13-17*a*, and points toward the binary face if three-phase reaction goes to higher temperature, Fig. 13-17*b*. Conversely, in the peritectic-type reactions, the tie-triangle points toward the binary side if the temperature of reaction decreases, Fig. 13-17*c*, and away if the temperature of reaction increases, Fig. 13-17*d*.

Some Details Concerning Three-phase Equilibrium

Any pair of binary three-phase equilibria that involve the same three phases may be joined in the ternary space model by a three-phase field composed of tie-triangles. This means that a binary eutectic may be joined with a binary peritectic, a eutectoid with a peritectoid, and a monotectic with a syntectic. Where a eutectic-type system is thus joined with a peritectic-type system (Fig. 13-18), the direction of the tie-triangle

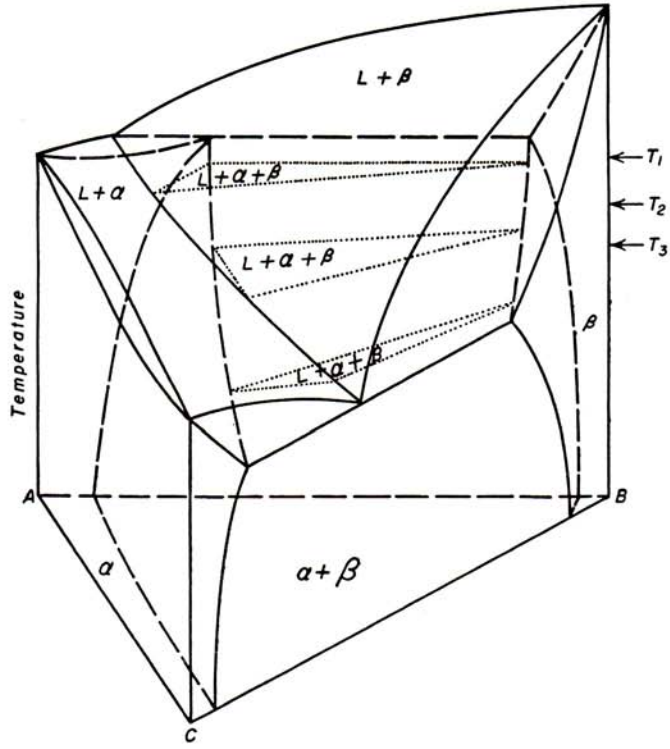

FIG. 13-18. Illustrating the rotation of the tie-triangle in passing between a binary eutectic and a binary peritectic.

changes in crossing the ternary space model. This is shown by the dotted triangles in Fig. 13-18 and also by the isotherms of Fig. 13-20. Alloys low in the A component will freeze by eutectic reaction, those low in the C component by peritectic reaction, and those of intermediate composition will follow a compromise course of freezing. In the present example, the intermediate alloys would at first exhibit some peritectic re-solution of the primary β constituent; this process would taper off to a reversal where the α and β phases are codeposited until the liquid is consumed. Since both phases of the secondary constituent in ternary alloys exhibit coring,

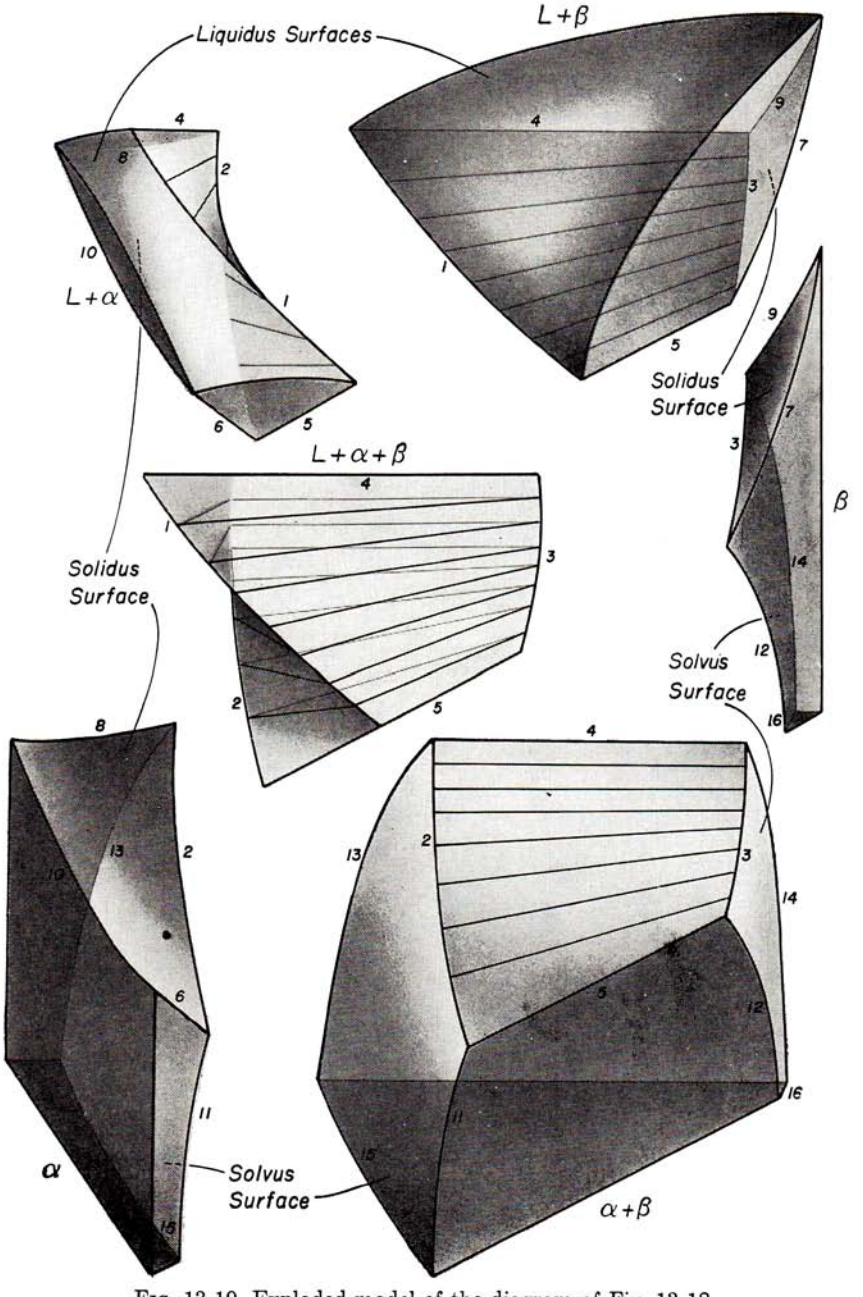

FIG. 13-19. Exploded model of the diagram of Fig. 13-18.

the appearance of the microstructure is altered gradually from the essentially eutectic- to the essentially peritectic-type alloys without any abrupt change of any kind.

The three-phase region of the space model has one face that turns through 180° in passing from one binary system to the other, the face

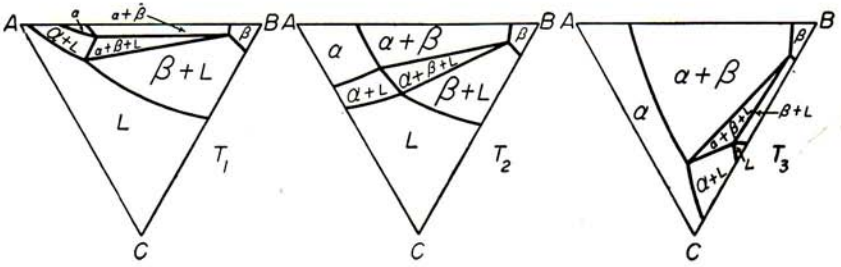

FIG. 13-20. Isotherms through the space diagram of Fig. 13-18.

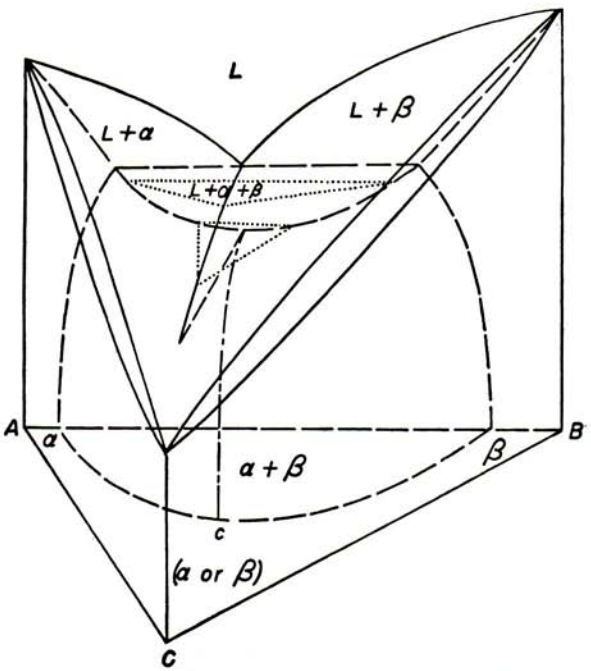

FIG. 13-21. Illustrating the termination of a three-phase equilibrium in a critical tie-line.

1-2-4-5 in Fig. 13-19. This surface is only partly visible in the drawing of the three-phase field, but the concealed portion can be seen in the drawing of the $L + \alpha$ field. In other respects this diagram closely resembles the two cases previously discussed.

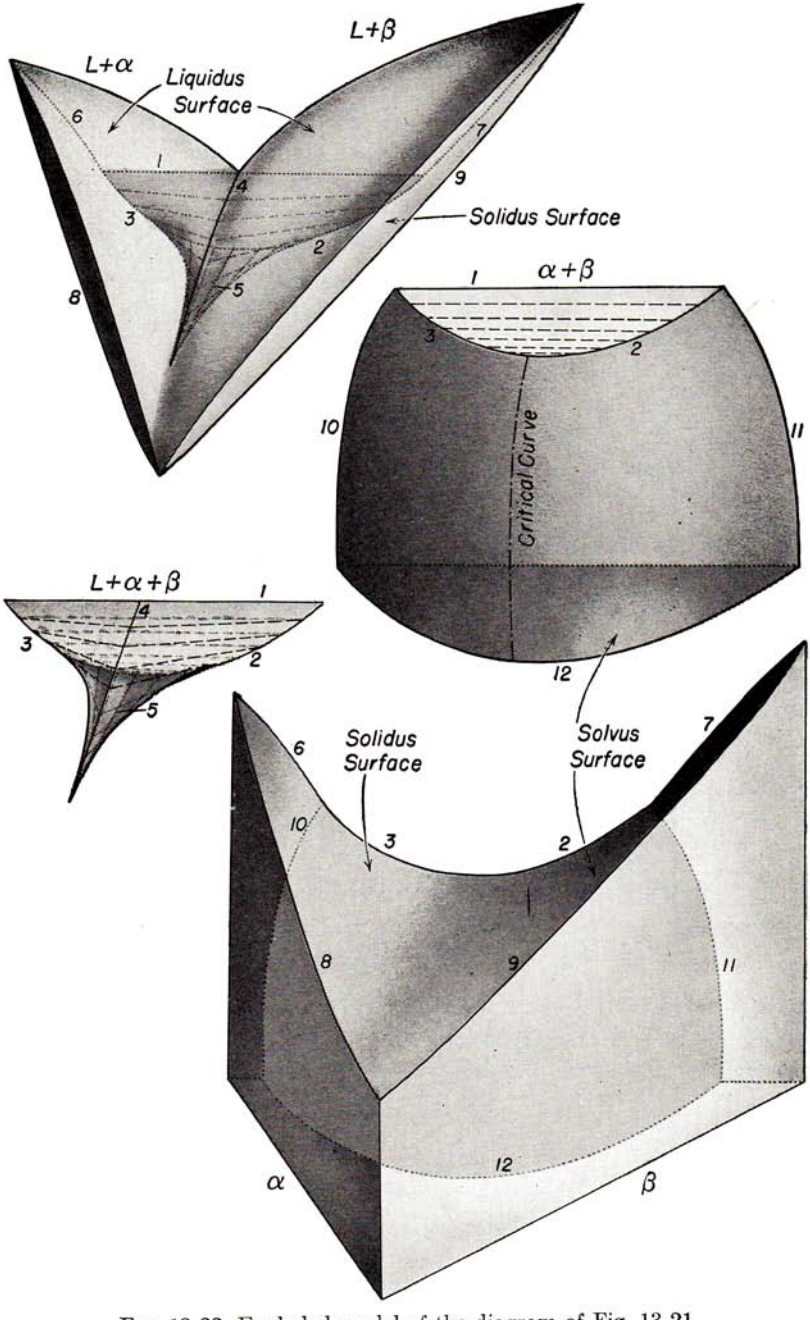

FIG. 13-22. Exploded model of the diagram of Fig. 13-21.

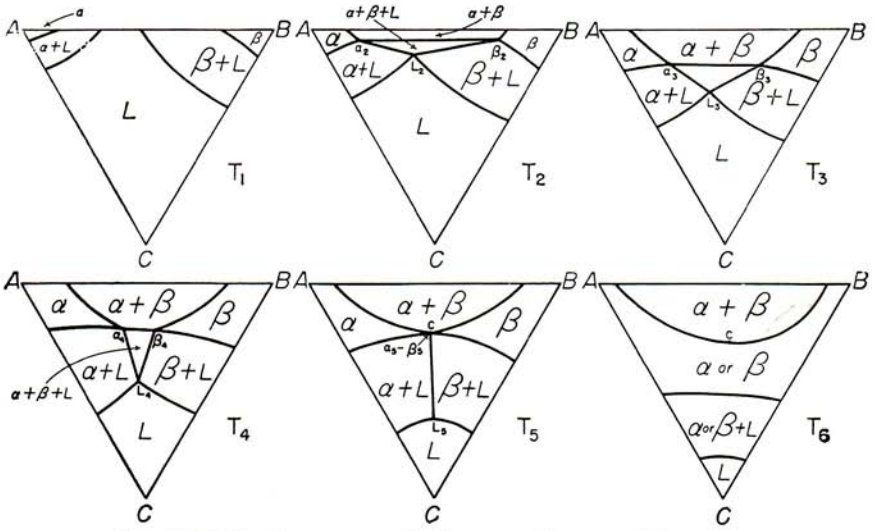

FIG. 13-23. Isotherms through the space diagram of Fig. 13-21.

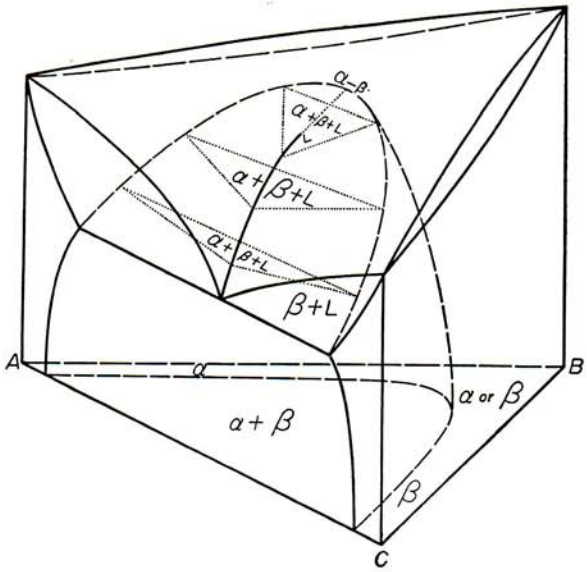

FIG. 13-24

In all the examples considered up to this point the three-phase region has terminated upon three-phase isotherms in the binary faces of the space model. There are two other ways in which the three-phase region may be terminated. One of these involves junction with a four-phase reaction, a subject which will be discussed in succeeding chapters; the

other is termination upon a critical tie-line in the ternary model (see Fig. 13-21). Here the $L + \alpha + \beta$ region begins upon the binary eutectic line, and the compositions of α and β approach each other as the temperature falls (Fig. 13-23) until, at a critical point c (T_5), the two solid phases become indistinguishable. In this way, the tie-triangle closes to a tie-line α_5-$\beta_5 L_5$ and the three-phase region ends.

The three-phase field of this example has two sharply curved surfaces, 1-3-4-5 and 1-2-4-5 in Fig. 13-22, and one surface of lesser curvature, 1-2-3. These join to produce a shape which is reminiscent of a bird's beak. The pointed part of the "beak" extends beyond the $\alpha + \beta$ region and penetrates the solid plus liquid field.

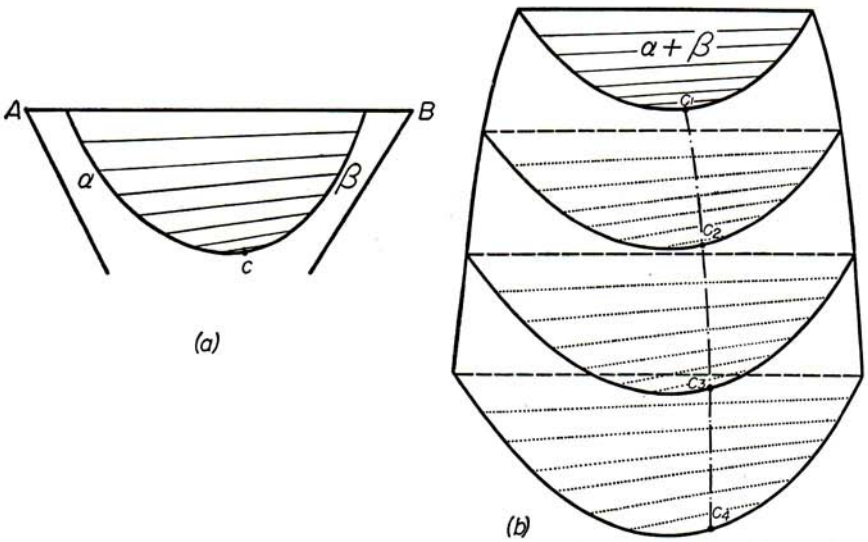

FIG. 13-25. A critical point occurs at c in each isotherm; the trace of the critical points in a series of isotherms produces the critical curve c_1c_4.

When the temperature of three-phase equilibrium rises as the composition recedes from the binary eutectic, the $L + \alpha + \beta$ field is inverted (Fig. 13-24) and ceases to resemble a beak; it terminates upon the tie-line $L\alpha$-β.

Critical Points and Critical Curves

It will be apparent that the merging of the α and β phases in the foregoing diagram corresponds to a critical point in two-phase equilibrium. At every temperature from T_5 downward in Fig. 13-23, the isotherm of the $\alpha + \beta$ field exhibits a critical point c, as is shown in detail in Fig. 13-25*a*. The tie-lines of the $\alpha + \beta$ field become progressively shorter as

the composition moves away from the AB side of the diagram, reaching zero length at point c, the *critical point*. Since there is a critical point at each temperature level in the two-phase field, these points trace a *critical curve* $c_1c_2c_3c_4$ in Fig. 13-25*b*, also shown as a dash-dot line on the boundary

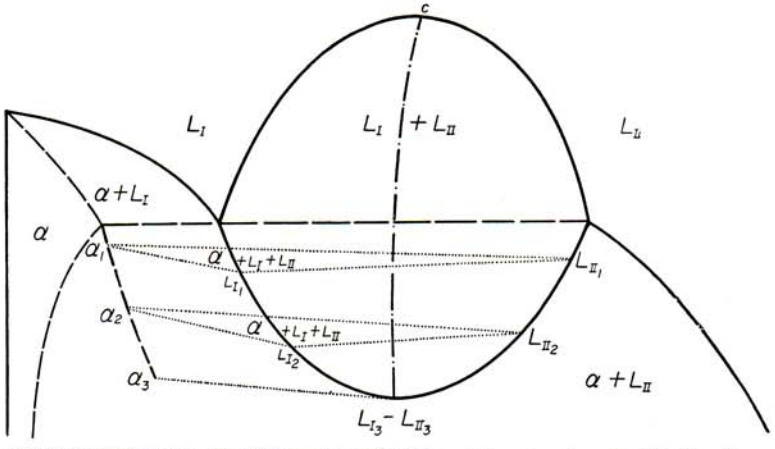

FIG. 13-26. Termination of a three-phase field involving two immiscible liquids and a solid phase at a critical point and tie-line.

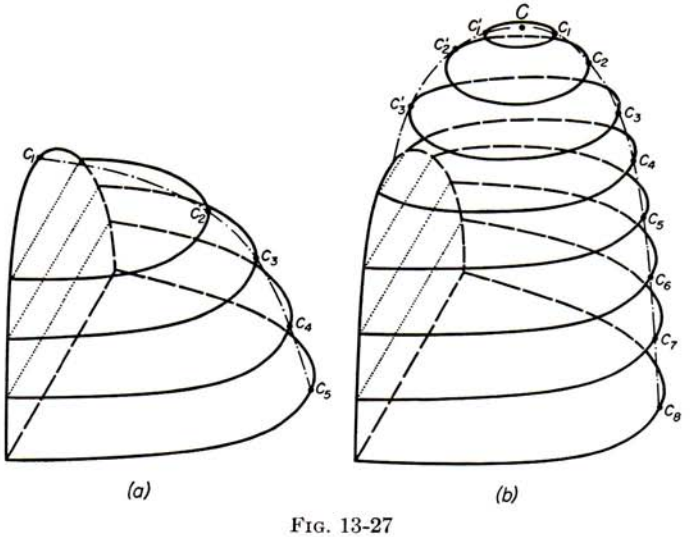

FIG. 13-27

of the $\alpha + \beta$ field in Figs. 13-21 and 13-22. The α and β phases are distinguishable only when they occur together in the $\alpha + \beta$ region or the $L + \alpha + \beta$ region. Elsewhere they form continuous series of solid solutions as in an isomorphous system. Obviously, the "two" solid phases must have the same crystal structure.

Another common example of the ending of a three-phase field upon a tie-line within the space model involves monotectic reaction (Fig. 13-26). Here the field $L_I + L_{II} + \alpha$ begins at the binary monotectic line and ends upon the tie line $\alpha_3 L_{I_3}$-L_{II_3}. Again the tie-triangle has closed to a line at a critical point L_{I_3}-L_{II_3}, where the two liquids become indistinguishable. The $L_I + L_{II}$ region in the space model has a critical curve cL_{I_3}-L_{II_3}.

It does not always happen that the highest point (temperature maximum) of the critical curve lies in a binary face of the space model; sometimes there is a ternary critical point which lies above the binary critical point. The two cases are illustrated in Fig. 13-27, where the "highest" critical point occurs in the binary face in drawing *a* and at point *C* within

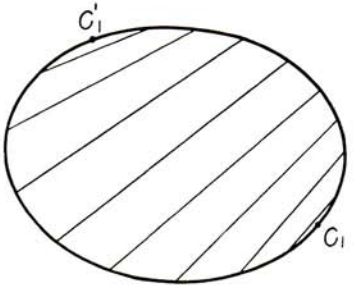

FIG. 13-28. Isotherm above the binary critical point in Fig. 13-27*b*.

the ternary space of the diagram in drawing *b*. In the latter case there are two critical points in each isotherm at any temperature lying between the ternary and binary critical points (Fig. 13-28).

Maxima and Minima

The three-phase region may pass through a maximum or minimum in temperature. When it does so, *the tie-triangle becomes a tie-line* connecting the three phases that are in equilibrium at the temperature maximum or minimum (Figs. 13-29 and 13-31). The details of these diagrams may be understood more easily by reference to the corresponding isotherms in Figs. 13-30 and 13-32. These examples involve only eutectic reaction; it is equally possible, however, to have maxima and minima with peritectic-type reactions or with combinations of eutectic- with peritectic-type reactions, and so on. Attention is directed to the analogy between the tie-triangle, which closes to a single line at a temperature maximum or minimum, and the tie-line of two-phase equilibrium which is reduced to a point at a temperature maximum or minimum, as in Fig. 12-18. In both cases the transformation assumes the form of a binary univariant reaction.

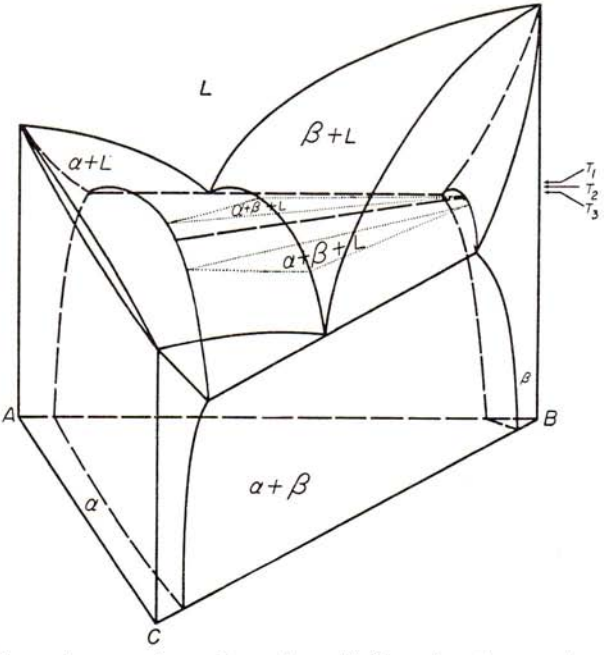

FIG. 13-29. Three-phase region reduces to a tie-line at a temperature maximum.

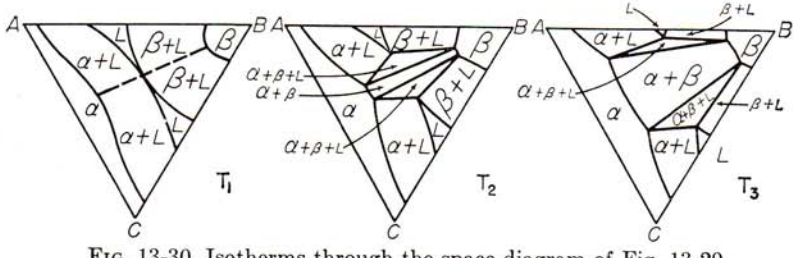

FIG. 13-30. Isotherms through the space diagram of Fig. 13-29.

Vertical Sections

Although bearing some resemblance to binary diagrams, vertical sections through the ternary space models discussed in this chapter have several very important differences that distinguish them from binaries. The reaction horizontal of the binary diagram is replaced by a three-phase region which has no fixed form, no straight or horizontal boundaries except by coincidence, and no definite number of bounding curves. Two simple cases are presented in Figs. 13-33 and 13-34. These sections correctly record the transformation temperatures for alloys having gross

compositions on the lines XB and WB, respectively; they do not, however, show the compositions of the phases involved in the corresponding equilibria, except in the one-phase fields. For example, an alloy of intermediate composition, held at a temperature within the $\alpha + \beta$ field, will

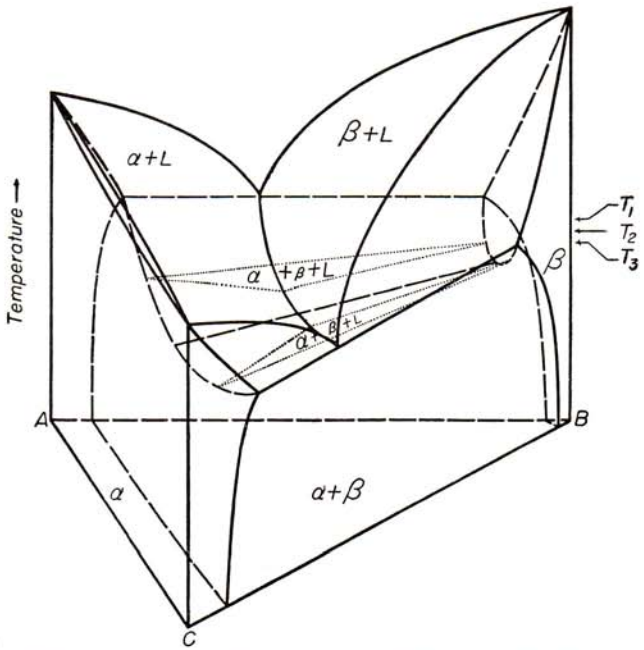

FIG. 13-31. Three-phase region reduces to a tie-line at a temperature minimum.

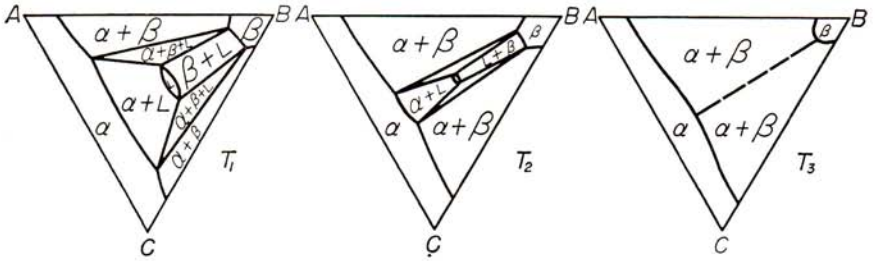

FIG. 13-32. Isotherms through the space diagram of Fig. 13-31.

be composed of $\alpha + \beta$, but the compositions of the conjugate phases cannot be read from the vertical section, nor can the lever principle be applied to ascertain the relative quantities of the two phases present at equilibrium. This situation is even more apparent in section YZ of Fig. 13-35, where the β phase is named in three different fields and yet does not appear, as such, at any point on the section. All compositions of β lie out-

side the composition range of this section. Another striking example of this is shown in Fig. 13-36. The section RS resembles section XB of Fig. 13-33, but in section TU the $L + \alpha + \beta$ field is entirely detached from the solid field and is bounded by a continuous line.

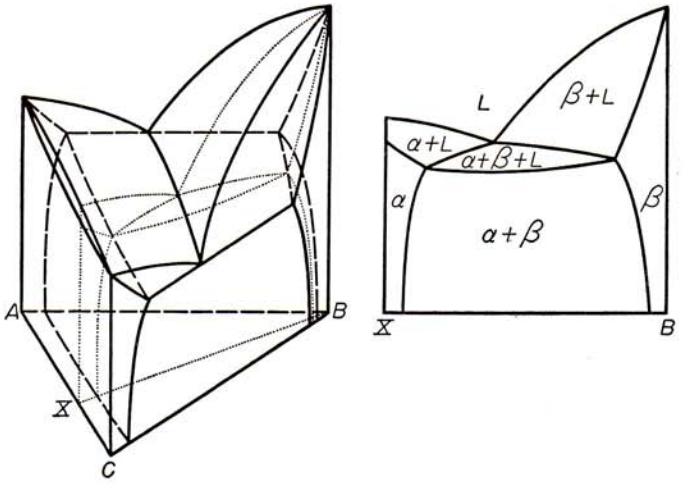

FIG. 13-33

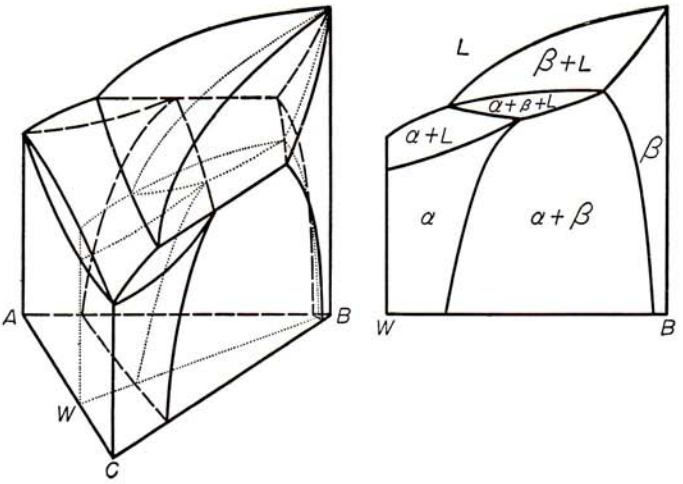

FIG. 13-34

Despite these disadvantages, vertical sections are usefully employed for the representation of portions of ternary alloy systems lying close to one of the binary sides of the space diagram. Many examples exist among iron-base ternary alloy systems. Of particular interest is the influence of a

third element upon the iron-carbon eutectoid reaction. With the first addition of a third element this reaction, of course, ceases to be isothermal, even under equilibrium conditions, but occurs over a temperature range.

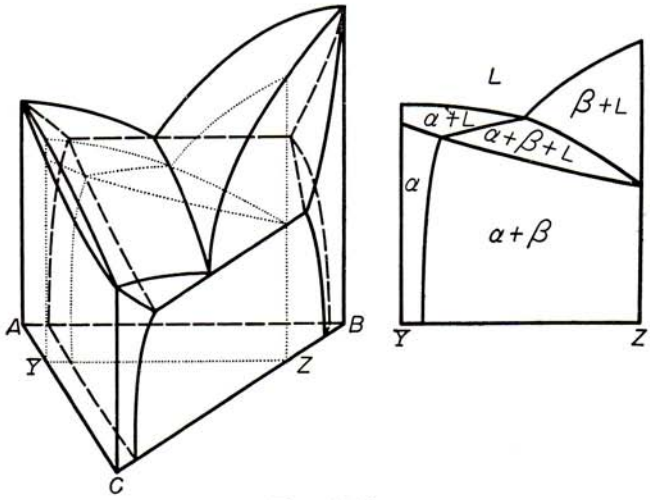

FIG. 13-35

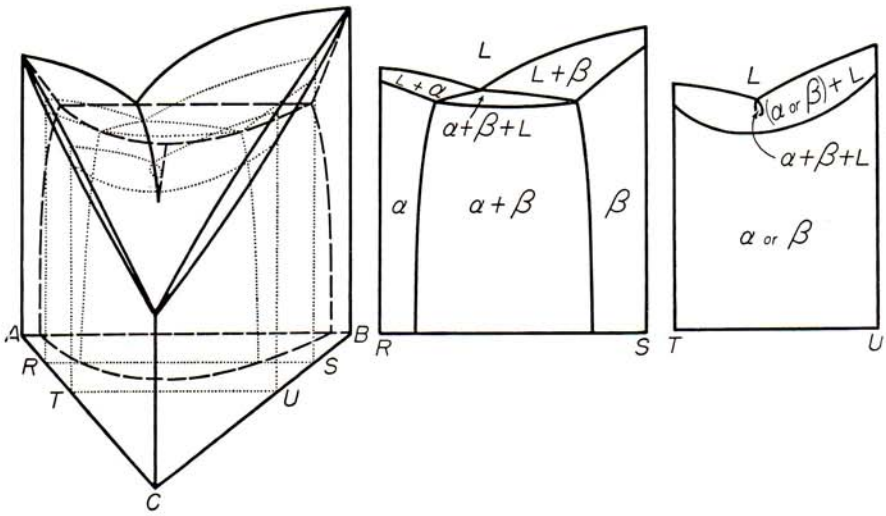

FIG. 13-36

The temperature range of transformation is elevated by some elements, lowered by others. These modifications change the rate of transformation, requiring a separate TTT curve for each individual alloy of each ternary alloy system.

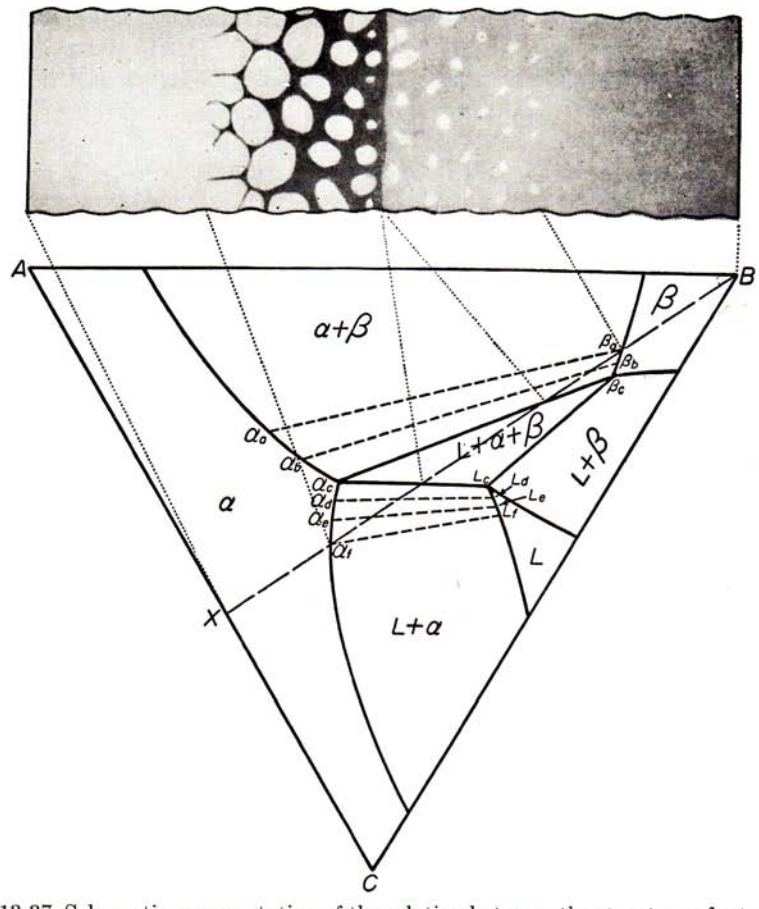

FIG. 13-37. Schematic representation of the relation between the structure of a ternary diffusion couple and the phase diagram. Layers are developed corresponding to both one- and two-phase regions lying upon the composition path between the extremes of composition; three-phase regions correspond to layer interfaces in the diffusion couple. The composition path of the diffusion couple is not usually straight as it is shown to be in this ideal example.

Isothermal Diffusion in Ternary Systems

Practical examples of approximately isothermal diffusion among three or more metals are far more numerous than those involving only two metals. Such processes as soldering, brazing, galvanizing, calorizing, oxidizing alloys at high temperatures, sintering complex metal powder mixtures, and many others involve substantially isothermal diffusion simultaneously among more than two metals. In view of its potential value, therefore, it is unfortunate that information with regard to the relation-

ships existing between ternary constitution and the structures produced by diffusion among three elements is very scanty. At the present time it is possible to say only that ternary diffusion can result in the formation of both one-phase and two-phase layers in a diffusion couple, but not three-phase layers. As with binary diffusion, no layers at all, but simply interfaces between layers, correspond to regions of divariant (or uni- or invariant) equilibrium.

These relationships are illustrated schematically in Fig. 13-37. A block of an alloy of composition X has been held in contact with a block of metal B, at the temperature of the isotherm, until diffusion layers have developed, as shown by the sketch above. It is assumed that all gross compositions that would be found by analyzing vertical slices through the diffusion sample, taken perpendicular to the plane of the drawing, would lie upon the line XB. This is known to be an erroneous assumption, but it provides the best approximation that can be made at present. The line XB crosses the fields α, $L + \alpha$, $L + \alpha + \beta$, $\alpha + \beta$, and β. Presumably, the α layer varies in composition from X to α_f and the β layer from β_a to B. The α of the $L + \alpha$ layer should then range in composition from α_f to α_c, and the conjugate liquid from L_f to L_c, while in the $\alpha + \beta$ layer the α should vary from α_c to α_a and the β from β_c to β_a. The $L + \alpha + \beta$ region is represented in the diffusion sample by the interface between the zones of $L + \alpha$ and $\alpha + \beta$. This course of reasoning is more or less successful in predicting the qualitative nature of "ternary diffusion structures," but it does not ordinarily predict the correct compositions of the several phases. In some cases where the diffusion velocities of the three components are markedly different, the path of composition change deviates radically from the direct path between the compositions of the end points.

Physical Properties of Alloys

Structurally, the ternary alloys of systems such as have been discussed in this chapter differ from the corresponding binary alloys chiefly in that "coring" is to be expected in cast ternary alloys in both the primary and secondary constituents. This may be expected to have only a minor influence upon the physical properties. The individual phases of the structure become ternary, rather than binary, solid solutions, and their particle sizes may be altered. These factors are capable of exerting a pronounced influence upon the physical properties, but no general principles governing the direction or magnitude of such effects are known at present. It might be supposed that adding a third element to each solid phase would be the equivalent of increasing the amount of material in solid solution and would, generally, increase the hardness and strength of the phase. This does not always happen, however, because the boundary surfaces of the

one-phase fields sometimes curve in such manner that the total quantity of substance in solid solution in a given phase is actually less in the ternary than in the binary alloys.

PRACTICE PROBLEMS

1. The binary systems AB and BC are both like that of Fig. 5-1, being isomorphous through the freezing range and of the eutectoid type at lower temperature. The binary system AC is isomorphous at all temperatures, i.e., both above and beneath the temperatures of allotropic transformation of A and C. Draw the space (TXY) diagram of the ternary system ABC; develop isotherms sufficient in number to display the main features of the internal structure of this diagram; develop isopleths through the B corner and also parallel to the AC side of the diagram.

2. Consider an alloy of gross composition near the mid-point of the eutectic valley in Fig. 13-21. Deduce the course of natural freezing of this alloy. In what ways might the cast alloy be expected to respond to heat treatment?

3. The binary system AC is isomorphous, the binary system BC is of the monotectic type, and the binary system AB is of the syntectic type. Draw a space diagram of the ternary system ABC, and check its validity by developing isotherms. The simplest solution of this problem results when it is assumed that the solid is isomorphous beneath the monotectic in BC and beneath the syntectic in AB. After solving the problem in this simpler form, substitute the binaries of Figs. 3-2, 6-1, and 10-1 and repeat.